The 100 years of AIChE: AIChE 2008 Annual International Conference, November 16-21, 2008 Loews Philadelphia Hotel, Philadelphia Marriott Downtown & Pennsylvania Convention Center Philadelphia, PA, USA

CFD Modelling Gas-Solid Flows in CFB/FCC Riser Reactors: Simulation Using Kinetic Theory of Granular Flow (KTGF) in a Fully Developed Flow Situation

M. N. Idris[1, 2] and **A. Burn**[3]
[1]School of Process Environmental and Material Engineering
University of Leeds, Leeds LS2 9JT, United Kingdom
[2]Dept of Chemical Engineering, University of Maiduguri, Nigeria
[*]Tel: +44-113-2160568, Email: chemni@leeds.ac.uk
[3]Multiphase Flow Programming Specialist
ANSYS UK Limited
United Kingdom

Abstract

This study presents the simulation of gas-solid hydrodynamics and flow behaviour in a riser in an FCC riser circulating fluidised bed (CFB) reactor using the Eulerian-Eulerian two-fluid modelling approach, incorporating a kinetic theory constitutive model for dilute assemblies of FCC particulate solid. The interaction between gas and particles was modelled using particle interphase transfer model and Gidaspow drag model on a proprietary computational fluid dynamics (CFD) code ANSYS CFX, using turbulent k-ε model. The interaction between gas and solid particles was modelled using particle interphase momentum transfer model with Miller-Gidaspow drag model on the commercial code. The simulation was run on steady state and then on transient conditions.

Computational fluid dynamics (CFD) usefulness for FCC riser reactor is reaching an advanced stage in solving real life problems. It is a good practise to run a time-average comparison for solid velocities and concentrations to measure fluxes and densities along the riser axes. However, the hydrodynamic behaviour of gas-solid flow in riser was successfully compared with published experimental data of a CFB/FCC riser of length 15.1m and 0.1 m diameter. The overall flow patterns within the riser bed were predicted well by the model. For volume fraction around 2-3%, which is the average particle concentration in the riser system, the computed solid-holdup agrees with the experimental measurements. The predicted results and analysis will be useful for further modelling of industrial FCC riser reactors.

Keywords: CFD, FCC, kinetic theory, hydrodynamic, two-phase, modelling, industrial application

1. Introduction

Circulating fluidised bed (CFB) reactors are widely used in the chemical and process industry to carry out a variety of multiphase gas-solid reactions. The extended use of fluidised bed equipment has opened wide possibilities for ensuring reliable design and improving various industrial technologies, which include: coal combustion and gas-solid catalytic reactions (gasification) such as fluid catalytic cracking (FCC) of long chain hydrocarbons, Fischer-Tropsch synthesis, maleic anhydride production, polymerization of olefins, coal gasification, incineration of solid waste, acrylonitrile production etc.

Fluid catalytic cracking (FCC) is a multibillion dollar worldwide industrial operation to converts heavy hydrocarbons (petroleum) to lower and more valuable molecular-weight products, such as gasoline. In the riser of a CFB, gas is passed through a bed of granular solid material at high velocities, which entrains the solids from the fluidised bed and transports them

out of the riser. Based on the bed structure and solid distributions along the riser height three distinct fluidisation regimes have been identified [1], namely: turbulent fluidisation, fast fluidisation and pneumatic conveying. Most industrial CFB reactors operate in the turbulent and fast fluidisation regime [2,3]. These fluidisation regimes are not fully understood [2, 4] and phenomenological flow models are not yet well established [1], consequently the reactor performance predictions are uncertain. Therefore there is a need for an enhanced understanding of the hydrodynamics of CFB in order to facilitate the reactor design and the selection of appropriate operating conditions to achieve the desired fluidisation regime. With recent advances in computational fluid dynamics (CFD) for multiphase flow, this approach can be used for the investigation of complex flow in CFB risers in a cost-effective way. However, such models require detail validation against data from large-scale experimental rigs before they can be used with confidence for the above purposes.

In the present study, gas-solid flow behaviour in the riser system of a CFB has been simulated using a proprietary CFD code [5]. The simulation is based on the experiments carried out by Huang et al. [6] in a pilot-scale FCC riser with 15.1m in height and 0.10m in diameter, which provided a sufficiently long distance for flow development. The solid used in the riser was FCC particles of 67μm mean diameter having density of 1500kg/m^3. The solid mass flow rate was varied between 50-200kg/m^{2}s. Air at ambient conditions was used in the experiment with superficial velocity varying between 3.5-8.0m/s. Figure 1 represents the schematic of the of the riser section of the CFB [6] simulated in this study. The CFD modelling methodology, embedded in the ANSYS CFX code [5], used in the calculation is based on the Eulerian-Eulerian multiphase flow model with constitutive equations for the gas-solid drag, solid stress, solid pressure, solid shear and bulk viscosity, and granular temperature. The solid pressure, shear and bulk viscosity were obtained in terms of granular temperature using the constitutive equation [5] derived from the kinetic theory of granular flow. Modelling of the hydrodynamics of gas-solid multiphase systems with Eulerain-Eulerian models using different CFD codes has shown the suitability of this simulation approach for modelling fluidised-bed reactors. The gas phase turbulence was handled using the k-ε model. Full details of the computational procedure are provided in the paper.

The computed results for solid circulation rates of 100kg/m^{2}s (with superficial gas velocities of 3.5 and 5.5 m/s) are compared with the experimental data [6] of radial distributions of particle concentration and mean velocity at 8 different locations along the height of the riser. The measured trends are generally well replaced in CFD predictions. In this work, detail comparisons between the predicted and measured particle velocities along the axis the radius at various height of the riser length measured from the inlet were presented.

2. Hydrodynamic Model Equations

The hydrodynamic model for the multiphase flow is based on the generalisation of Navier-Stokes equations, which uses Eulerian-Eulerian approach [7]. The Eulerian-Eulerian approach is particularly suitable to simulate industrial bubbling/turbulent riser bed reactors (which may contain billions of solid particles). These equations use granular kinetic theory for the particulate phase. The basic fundamental equations given below are the mass, momentum and energy conservation laws for the fluid and the particulate phases. The CFD modelling methodology, embedded in the ANSYS CFX code [5], used in the calculation is based on the Eulerian-Eulerian multiphase flow model with constitutive equations for the gas-solid drag, solid stress, solid pressure, solid shear and bulk viscosity, and granular temperature. The solid pressure, shear and bulk viscosity were obtained in terms of granular temperature using the constitutive equation [5] derived from the kinetic theory of granular flow. This model is used in this study with the modified Wen and Yu drag law, as in [8]
The gas phase turbulence was handled using the k-ε model.

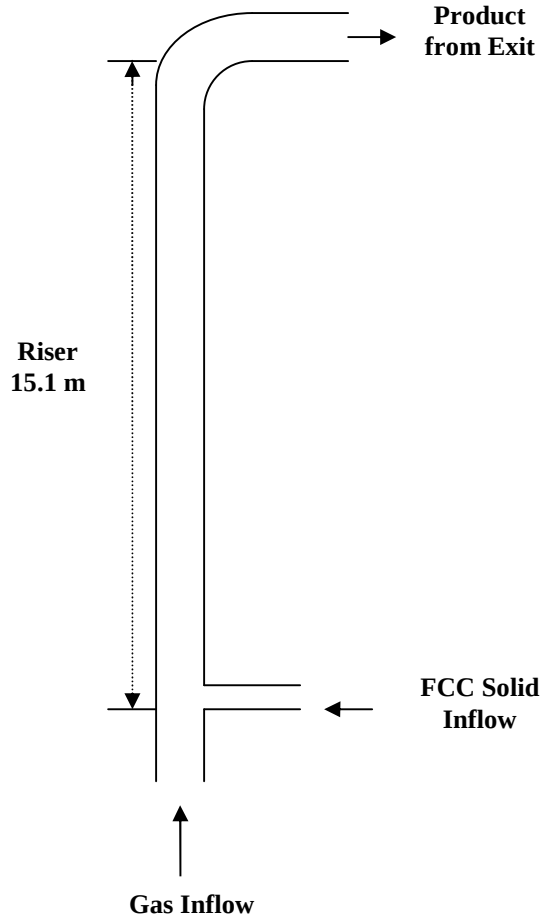

Figure 1 Schematic diagram of a CFB/FCC riser system. The riser is of length 15.1 m and 0.1 m in diameter.

In the 21st century, engineers want to do better still. Why? Because increasing the production of desired product by 1% would increase the profit per reactor by $1 to $2 million/year [1]. Again, due to increase in energy cost and depleting petroleum resources, there is a need for FCC riser optimisation. Equally, the quest is to optimize FCC riser reactor using CFD in order to improve efficiency, cost, environmental impact and health and safety of managing manpower of the process plant. The best use of this commercial software is the flexibility of varying parameters to optimise the simulation solution.

2.1 The governing conservation equations

The continuity equation for gas phase total mass balance is given by

$$\frac{\partial}{\partial t}\left(\varepsilon_g \rho_g\right) + \nabla.\left(\varepsilon_g \rho_g \vec{v}_g\right) = 0 \tag{1}$$

Solid phase continuity

$$\frac{\partial}{\partial t}\left(\varepsilon_s \rho_s\right) + \nabla.\left(\varepsilon_s \rho_s \vec{v}_s\right) = 0 \tag{2}$$

The volume fraction balance equations is (φ=g, s)

$$\varepsilon_g + \varepsilon_s = 1 \quad \text{or} \quad \sum_g r_g + \sum_s r_s = 1 \tag{3}$$

Where ρ is the density of each phases, ε is the volume fraction, and $\vec{v}$ is the velocity vector

Momentum equations

The mass conservation equations for phase (φ=g, s) is

$$\frac{\partial}{\partial t}\left(\varepsilon_\varphi \rho_\varphi\right)+\nabla\bullet\left(\rho_\varphi \varepsilon_\varphi \vec{v}_\varphi\right)=0 \tag{4}$$

Momentum conservation gas-phase

$$\frac{\partial(\varepsilon_g \rho_g U_g^i)}{\partial t}+\frac{\partial(\varepsilon_g \rho_g U_g^j U_g^i)}{\partial x^j}= \quad -r_g\frac{\partial P_g}{\partial x^i}+\frac{\partial(\varepsilon_g \tau_g^{ij})}{\partial x^j}+\varepsilon_g \rho_g g^i + M_g^i \tag{5}$$

Momentum conservation solid phase

$$\frac{\partial}{\partial t}\left(\varepsilon_s \rho_s\right)+\nabla.\left(\varepsilon_s \rho_s \vec{v}_s\right)+\nabla.\left(\varepsilon_s \rho_s \vec{v}_s \vec{v}_s\right)=\nabla \vec{T}_s-\beta_B.\left(\vec{v}_s-\vec{v}_g\right)+\varepsilon_s\left(\rho_s-\rho_g\right)\vec{g} \tag{6}$$

Where P is the pressure, $\vec{T}_g$, $\vec{T}_s$ are the stress tensors, β is the interface momentum transfer coefficient, and g is the acceleration due to gravity. Hence, $\vec{v}_{gs}$ is the interphase velocity and $\varepsilon_s\left(\rho_s-\rho_g\right)\vec{g}$ is an interaction force between phases. $\bar{\tau}$ is the φ_{th} phase Reynolds stress tensor

$$\tau=\varepsilon_\varphi \mu_\varphi\left(\nabla \vec{v}_\varphi+\nabla \vec{v}_\varphi^{\,T}\right)+\varepsilon_\varphi\left(\lambda_\varphi-\frac{2}{3}\mu_\varphi\right)\nabla\bullet\vec{v}_\varphi I \tag{7}$$

Hence, μ_φ and λ_φ are the shear and bulk viscosity of phase φ, respectively, and *I* is the unit tensor. The solid pressure, P_s, solid shear viscosity λ_s, are calculated from the kinetic-frictional stress model discussed in the following section.

Constitutive equations

The ideal gas law is applied to determine the gas pressure where T is the temperature, but this is a cold flow simulation where ambient conditions are applied. Then is the gas phase, the pressure of the gas is given as:

$$P_g=\rho_g \bar{R}T \tag{8}$$

Assuming a constant density case, the solenoidal total volume flux is given as in [9]

$$\frac{\partial}{\partial x^j}\left(\sum_g r_g U_g^j\right)+\frac{\partial}{\partial x^i}\left(\sum_s r_s U_s^i\right)=0 \tag{9}$$

Interphase momentum transfer

The drag on single particle expressed in terms of dimensionless drag coefficient is given as:

$$D = \frac{1}{2} C_D \rho_f A_p \left| U_f - U_p \right| \left(U_f - U_p \right) \tag{10}$$

Where C_D is the non-dimensional drag coefficient of the gas-solid flow. Assuming that the solid particles are of fixed diameter, and then the volume of single particle is given as:

$$V_P = \frac{\pi d_p^3}{6} \tag{11}$$

$$S_P = \frac{\pi d_p^2}{6} \tag{12}$$

Then the number of particle per unit volume is given as:

$$n_p = \frac{\text{volume occupied by particles in unit cell}}{\text{volume single particle}} \tag{13}$$

$$\Rightarrow n_p = \frac{r_p}{V_p} = \frac{6 r_p}{\pi d_p^3} \tag{14}$$

And

$$\mathrm{Re}_{\alpha\beta} = \frac{\rho_{\alpha\beta} \left| \underline{U}_\beta - \underline{U}_\alpha \right| d_{\alpha\beta}}{\mu_{\alpha\beta}} \tag{15}$$

2.2 Kinetic theory of granular flow

The granular temperature models are based on the interpenetrating continuum assumption. Both gas and solid phases are modelled as a continuum. In this approach, individual particle trajectories are not simulated but an attempt is made to represent physics of those trajectories and particle-particle interactions using averaged form of governing equations. Due to the use of such averaged equations, models based on this approach can be extended to simulate gas-solid flows comprising large number of solid particles. In this industrial code, the algebraic equilibrium approach was computed by the solver using Gidaspow correlation for the radial distribution on the FCC solid particles. The solid shear viscosity, the solid pressure model and the solid bulk viscosity were computed as a function of granular temperature. For granular flows in an incompressible regime (i.e., where the solids volume fraction is less than its maximum allowed value), a solids pressure is calculated independently and used for the pressure gradient term. According to the granular kinetic theory, the kinetic energy of granular mean flow first degrades in the kinetic energy of random particle fluctuations, and then dissipates as heat of inelastic collisions [9].

Following Lun et al's theory, the kinetic energy of fluctuations is accounted for in the granular kinetic theory by defining a granular temperature Θ_s:

$$\Theta_s = \left\langle c^2 \right\rangle / 3 \tag{16}$$

Where c is the particle fluctuating velocity. Thus, the granular temperature for the solid phase is proportional to the kinetic energy of the random motion of the particles.

2.3 The Algebraic Equilibrium Model

ANSYS CFX is restricted to models where the granular temperature Θs is determined algebraically. Previous work has shown that direct adoptions of the default Eulerian-Eulerian models available in FLUENT or CFX, the simulation may not give right predictions on hydrodynamics [10]. Effort is on-course in CFX where granular temperature is determined using transport equation model, using the UDF (user-defined function). The Algebraic Equilibrium model has the flaw that unphysically large granular temperatures can be generated in regions of low solid particle volume fraction. To circumvent this, it is recommended that we specify an upper bound for the granular temperature. The Zero Equation Model implements the simpler algebraic model of Ding and Gidaspow [7] was applied in this simulation and is given as:

$$\Theta_s = \frac{1}{15(1-\varepsilon)} d_s^2 \cdot S^2 \tag{17}$$

Eqn (17) is based on the algebraic equilibrium with the rate of production equal rate of dissipation energy, and is represented as follows:

$$\text{Pr}\,oduction = Dissipation \Rightarrow \tau_{sij} \frac{\delta U_i}{\delta x_j} = \gamma_s \tag{18}$$

Where τ_{sij} denotes the solids shear tensor.

$$\gamma_s = 3(1-e^2) r_s^2 \rho_s g_0 \Theta_s \left[\frac{4}{d_s} \left(\sqrt{\frac{\Theta_s}{\pi}} - \frac{\delta U_k}{\delta x_k} \right) \right] \tag{19}$$

The restitution coefficient r_{coeff} for particle collisions and g_0 is a radial distribution function and can be seen as a measure for the probability of inter-particle contact and expressed by [10]:

$$g_0 = \left[1 - \left(\frac{\varepsilon_s}{\varepsilon_{s,\max}} \right)^{1/3} \right]^{-1} \tag{20}$$

Where $\varepsilon_{s,\max}$ is the maximum particle packing

Recently, [11] showed that this for the radial distribution function agrees with experimental data for FCC particles. Furthermore, in effort to resolve the fluctuating energy equation, we need to specify the conductivity of the particle fluctuating energy, *k*, and the collisional rate of energy dissipation per unit volume, γ

$$\gamma = 3(1-e^2) \in_s^2 \rho_s g_0 \Theta \left[\frac{4}{d_s} \left(\frac{\Theta}{\pi} \right)^{1/2} - \nabla \cdot v_s \right] \tag{21}$$

The gas-solid drag coefficient for different solid concentrations as presented in [11] as follow:

For $\in_g \geq 0.8$:

$$\beta = \frac{3}{4} C_d \frac{\in_s \rho_g \left| v_g - v_s \right|}{d_s} \in_g^{-2.65}, \tag{22}$$

where the drag coefficient C_d is given by

$$C_d = \frac{24}{\mathrm{Re}_s}\left(1 + 0.15\,\mathrm{Re}_s^{0.687}\right); \qquad \mathrm{Re}_s < 1{,}000 \tag{23}$$

$$C_d = 0.44; \qquad \mathrm{Re}_s \geq 1{,}000 \tag{24}$$

$$\mathrm{Re}_s = \frac{\in_g \rho_g d_s \left| v_g - v_s \right|}{\mu_g}, \tag{25}$$

For $\in_g < 0.8$:

$$\beta = 150 \frac{\in_s^2 \mu_g}{\in_g^2 d_p^2} + 1.75 \frac{\rho_g \in_s \left| v_g - v_s \right|}{d_s \in_g}, \tag{26}$$

2.4 Interphase momentum transfer

For an inhomogeneous phase, the interphase momentum transfer, M_{gs}, occurs due to interfacial forces acting on each phase, due to interaction with another phase β. The total force on phase *g* due to interaction with other phases is denoted M_g, and is given by:

$$M_g = \sum_{s \neq g} M_{gs} \tag{27}$$

Note that interfacial forces between two phases are equal and opposite, so the net interfacial forces sum to zero.

2.4.1 Initials and boundary conditions

The definition of appropriate initial and boundary conditions is critical and important for carrying out of a realistic simulation. The system conditions studied are those in [6] and are represented in Table 1 below.

1) At the initial condition, the riser column was assumed empty, and the velocity of both gas and FCC particles were set to be 3.5m/s with 100kg/m^{2}s solid loading (first case) and 5.5m/s with 100kg/m^{2}s solid loading (second case).
2) At the outlet, average static pressure of zero was set, based on the atmospheric inlet reference pressure. Particularly important is also the specification of appropriate boundary conditions at the wall (default domain).
3) Along the wall, a no-slip boundary condition was applied and free-slip for particles was used. A smooth wall influence was based on fluid dependence flow.

Table 1 Inlet, outlet and boundary conditions used in the simulation

Parameter	Case I	Case II	Case III*
Inlet conditions:			
Solid mass flux (kg/m^{2}s)	100	100	200
Solid velocity (m/s)	3.5	5.5	5.5
Gas superficial velocity (m/s)	3.5	5.5	5.5
Air volume fraction (dimensionless)	0.9813	0.9906	0.9763
Solid volume fraction (dimensionless)	0.0187	0.0094	0.0227
Outlet conditions:			
Pressure boundary conditions	0.0	0.0	0.0

*Case III was not reported in this paper

4) An outlet boundary opening is set for the outflow, to prevent overflow using a convenient transient simulation approach.
5) Global initialisation was done based on Cartesian velocity component having values of u=0, v=0 and w=3.5 and the 5.5m/s at reference volume fraction of air.

2.5 Computational domain and scope

The simulations were carried out for the riser section of the circulating fluidised bed shown in Fig. 1. A 3-D ANSYS CFX-Design modeller was used in developing the grids according to some specification from [9]. The system geometry and system properties are defined in Table 1. An unstructured grid was used throughout of a limiting case of a multi-block grid where each individual cell is treated as a block. The advantage of this arrangement is that there is no implicit structure of co-ordinate lines imposed by the grid. Fig. 1. is a three-dimensional Cartesian coordinates system used. The system geometry and system properties are defined in Table 2. In this study, the restitution coefficient of 0.99 was used. Previous studies have given a range of 0.80-0.99. The restitution coefficient is an empirical input in the kinetic theory based CFD model.

Table 2 Experimental conditions in the fluidised bed riser used by [6]

Parameters	Description	Experiments	Simulation
ρ_g (kg/m^3)	Gas density	Not specified	1.185
ρ_s (kg/m^3)	Solid density	1500	1500
μ_g (kg/ms)	Gas dynamic viscosity	Not specified	1.831E-05
μ_s (kg/ms)	Solid viscosity	Not specified	1.00E-05
d_p (μm)	Particle diameter	67	67
r_{coeff} (dimensionless)	Particle restitution coefficient	Not specified	0.99
d_i (m)	Riser diameter	0.10	0.10
h_i (m)	Riser height	15.10	15.10

2.6 Solution procedure

The set of governing equations in section 2.1 – 2.4 was solved by finite control volume technique. Miller-Gidaspows' drag model option was chosen in the CFD input code (CFX11.0). The properties of gas and FCC particles such as specific heat, viscosity, are temperature and composition dependent. The coefficient of restitution is an empirical input in the kinetic theory based CFD model. It is obtained by matching the experiment with the theory. A simulation of high coefficient of restitution

Grid dependency study is the best application method that makes numerical simulation complete. In this work, the grid dependence is tested by varying the mesh numbers and the time step was kept to meet the courant number requirement. The typical values of under relaxation factors between 0.06 – 0.27 were set as default in the solver.

Advection scheme of high resolution was set based on steady/unsteady state scheme using second backward Euler simulation. A residual type convergence criterion, RMS having a target of 1.0E-04 was used.

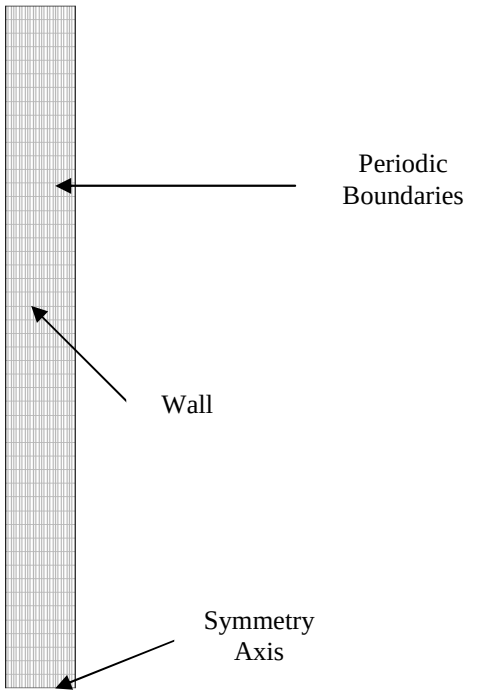

Figure 2. Straight pipe unstructured Mesh

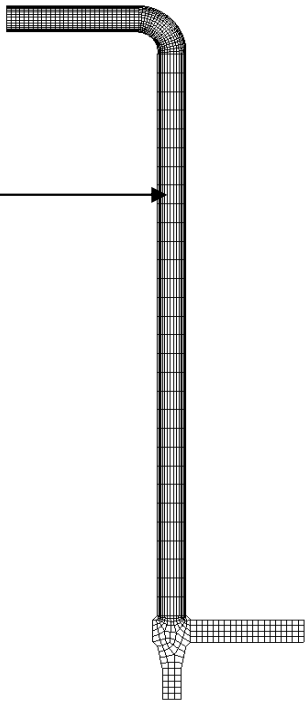

Figure 3. Riser pipe bend Mesh

3. Simulation

The simulation model basically consists of a turbulent flow, where two phases enter into contact: a gas phase formed by ideal gas at 25^0C and a particulate FCC solid phase composed of catalyst properties. The particles are considered smooth, spherical and inelastic, with an average diameter of 67μm and a density of 1500 kg m^{-3}. Table 1 and 2 shows the details of the feed properties input into the riser system.

Boundary conditions

At the entrance, all velocities and concentrations of both phases are specified. The set-up was based on atmospheric condition of temperature and pressure, fluid treated as incompressible. At the initial conditions, the superficial gas velocity is specified at 3.5 m/s (Case 1) and 5.5 m/s (case 2). At the walls, the gas velocity is zero; the FCC particle phase velocity has a no-slip condition.

Mesh and computational code

An unstructured mesh is composed of 156,000 control volumes, 476,690 faces and nodes 164,892. The details of its refinement, both at the entrance and at the exits, are presented in Figs 2 and 3. The time step is on the order of 10^{-4}s. Adaptation of the mathematical model for the numerical model generation was achieved with the ANSYS CFX 11.0 commercial simulator, which is based on the finite volume method, incorporating the high resolution scheme.

In the dependency evaluation of the flow with the numerical mesh, it is known that an adequate number of control volumes are of extreme importance to avoid numerical errors, which is not possible with less refined meshes. Thus, five meshes, with 133,495, 156,000, 596,964, and 985,265 and 1,334,925 control volumes respectively, were tested. The mathematical-default model used in accordance with the practice normally adopted, i.e., the flow inside the riser equipment is purely gaseous (ideal gas), subjected to the conservation equation of continuity and momentum for each phase. The simulations with different meshes resulted in the following observations:

- *Axial dependency* (r = 0 m and z = 0 – 14.08 m): There was no much significant influence on the mesh refinement in the axial direction. However, a noticeable variation was verified in the less refined mesh in the feed contact region, which is considered a critical point in the experimental case studied.
- *Redial dependency* (z = 0.95 m): In this transverse section, practically in the feed contact region, the radial behaviour of the flow is analogous to that described for the axial dependency.
- *Redial dependency* (z = 8.16 m): In this section, an insignificant influence of the refined mesh was also observed; all meshes provided the same qualitative profile and quantitative profile.
- *Redial dependency* (z = 14.08 m): Dependency on the refined mesh was more noticeable toward the exit section, even with clear difference observed. However, this does not modify the qualitative results.

Then the mesh composed of 156,000 control volumes was chosen; this was shown to be in accordance with the established standards (that is, there is no significant difference between the calculated flow of this mesh and those of the refined ones), when compared with the predictions from the other meshes.

4. Results and Discussion

Initially the numerical meshes were tested done and the one that had the best behaviour in the standard flow was used to run the simulations for the real process. The particle velocity radial profiles for the CFB/FCC risers were analysed, using the same conditions from the experimental studies reported. Thus, the report of [11] has show a good agreement between model predictions and experimental data of [12]. Instead of repeating those simulations, in this work, we have simulated gas-solid flow corresponding to experimental conditions of [6]. In order to determine the validity of these models, the simulation results are compared with experimental data using same input variables in the tests as the simulation program input. Quite a number of simulations have been performed in order to investigate the effect of different operating conditions, model assumptions, and to get an accurate description of the observed gas-solid phase flow pattern in the riser. The main interest here is on the solid phase volume fraction distribution, velocity distribution of both phases, granular temperature, FCC viscosity and solid hold-up.

Table 3: ANSYS CFX-Pre input simulation setup

Model	Parameters	Values and Comment
	Simulation Type:	Steady state/Transient Simulation
Fluid:	Fluid list:	Air at 25^0C and FCC Particles
	Reference pressure:	1-atm
	Buoyancy option:	Buoyant
	Domain motion:	Stationary
	Fluid models:	*Eulerian-Eulerian* Non-homogeneous model
	Turbulence model:	k-ε model
	Fluid details:	Ideal Air and FCC Particles Air at 25^0C as continues fluid FCC Particles as dispersed solid
	FCC Particle mean diameter:	67μm
	Restitution coefficient:	0.99
	Kinetic Theory:	Granular Temperature Model: *Algebraic equilibrium*
	Model option used	Miller-Gidaspow
	Radial Distribution Function:	Kinetic Theory
	Solid Pressure Model:	Kinetic Theory
	Solid Bulk Viscosity:	Kinetic Theory
	Solid Shear Viscosity:	Kinetic Theory
	Interphase transfer:	Particle Model
	Drag force used	Gidaspow
Fluid Default:	Wall influence on Flow:	Fluid dependent
	Wall Roughness:	Smooth wall
	Wall contact model:	Volume fraction used
	Air at 25^0C:	No slip
	FCC Particles:	No slip/Free slip
Fluid Inlet	Fluid Region:	Subsonic: Normal Speed: 3.5 and 5.5 m/s Solid Concentration: 100 kg/m^{2}s
	Air volume fraction:	0.9813 (dimensionless) at 3.5m/s
	FCC Particle volume fraction:	0.0187 (dimensionless) at 3.5m/s
	Turbulence Intensity:	Medium: 5%
Fluid Outlet (Opening)	Fluid Region:	Subsonic:
	Mass and momentum:	Average Static Pressure: 0.0Pa
	Turbulence:	Zero gradient
Solver control:	Discretization (Advective) scheme:	High Resolution
	Transient scheme:	Second order Backward Euler
	Convergence Criteria:	RMS
	Residual target:	1.0E-04
	Equation class setting:	Continuity
	Time step (Residual Target):	1.0E-4s
	Total Time:	40-secs

4.1 Gas phase distribution (single phase)

The initial setup case was based on gas (single) flow in the riser domain. The results were to prove the capability of the solver code in term of the turbulence modelling of the flow. The results were found to be in agreement with the 1/7th power law profile as observed by [12] and [13]. Fig 4 and 5 show the time-mean single phase turbulent velocity profile achieved in the initial set case. At the inlet axis of the riser, there was a uniform velocity flow which subsequently developed to turbulent flow regime [14]. Fig 5 shows the further development of the flow into a fully developed regime. The riser is of total length 15.1m, but the velocity comparison with the experimental case was based on the probe point of 14.08m. These flows were compared favourably with the $1/7^{th}$ power law profile based in basic fluid dynamic flow [15].

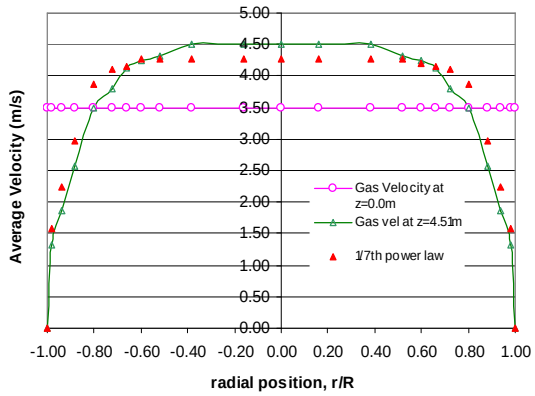

Fig 4. Gas velocity profile at z =0.0m and 4.51m

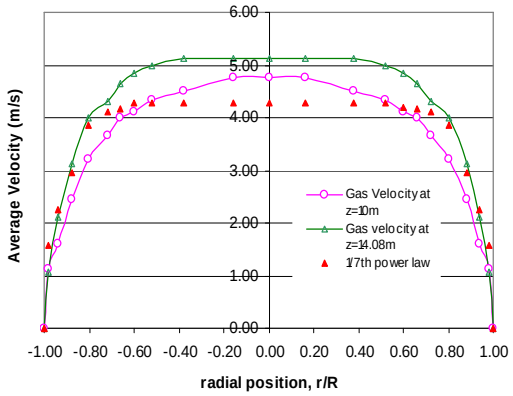

Fig 5. Gas velocity profile at z = 10m and 14.08m

Fig 6 shows axial profiles of cross-sectional average solids holdup in both the 15.1 m and 10 m heights. In this figure, its vivid that the distribution in the riser are uniform except at the inlet region. The solid distribution at the entrance region is highly influenced solid structure. The fully developed region in the 10 m riser is much lower than that of the 15.1 m. Thus, the riser height is of great importance to the solids distribution. From Fig. 6, it's clear that the decrease in the superficial gas velocity results to increase in the cross-sectional average solids holdup, while increasing solids fluxes increases the cross-sectional average solids holdup which has been shown in previous studies [15, 16].

4.2 Axial Distribution of Solids Holdup in the FCC riser

Fig. 6 represents the axial distribution profile of cross-sectional solids holdup in the CFB/FCC riser of height of 15.1 m. A summary of this riser is shown in Fig. 1. I n the simulation setup case, the solids circulation rate was set to be 100 kg/m^{2}s on a varying superficial gas velocity between 3.5 m/s and 5.5 m/s. It is very clear from Fig. 6, that there is uniformity in axial distribution in the riser system. The non-uniformity is shown at the entrance region of the riser. The factor that influences the solids distribution is basically the distribution structure, which has been seen in previous studies [6]. Therefore, the riser height is important to the solids distribution in CFB/FCC riser system. From Fig. 6, it is shown that decreasing the superficial gas velocity result an increase in cross-sectional average solids holdup and vice versa [6].
Figs. 7 and 8 represent the contour plot at the upper-end of the riser system. Fig. 8 show the vector plot of the flow while Fig. 9 represent the contour plot of the injection-mixing section in the riser system.

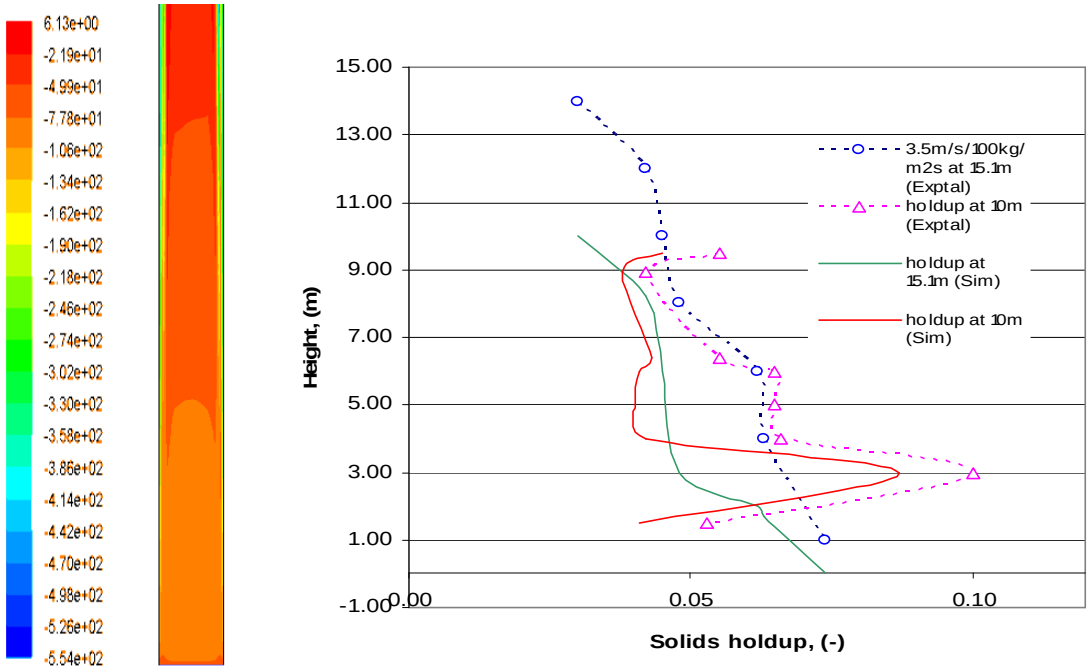

Fig 6. Comparison of axial solids holdup at various heights with contour plot of FCC Particle flow

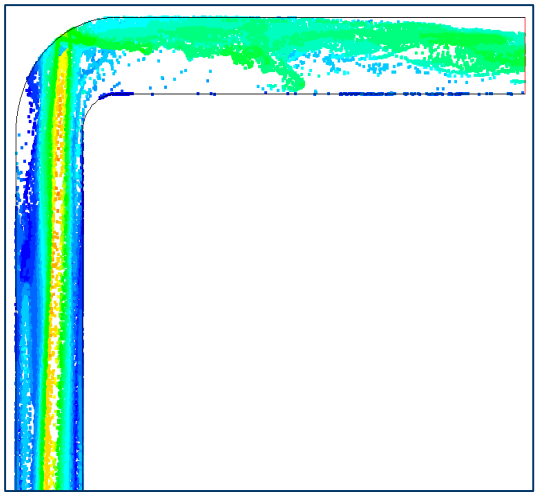

Fig 7(a). Contour plot of FCC Particle flow in the riser

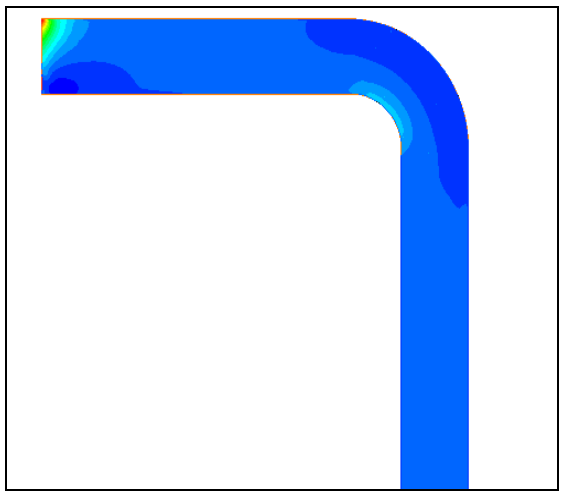

Fig.7(b). Contour of upper bend section (gas-phase)

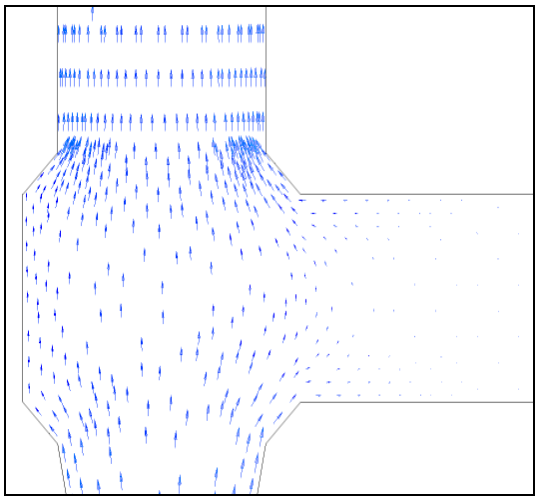

Fig 8. Vector plot of the injection-mixing section

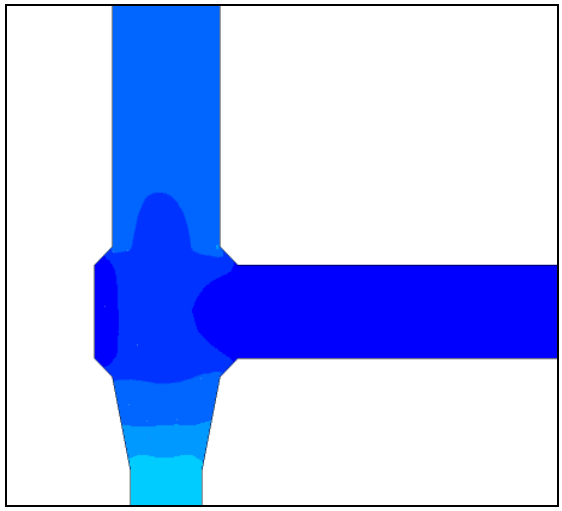

Fig.9. Contour plot of the injection-mixing section

4.3 FCC Solid Velocity distribution of both gas-solid phases

In developed flow, the slip velocity is approximately the terminal velocity. For the Geldart A particles (e.g. FCC particles at 1500kg/m^3), the solid velocity is close to the gas velocity in the direction of flow. A balance between buoyancy and drag obtained from the basic momentum balances for one-dimensional, developed flow is as follows:

The simulations carried out throughout this research showed that in each one of the transversal sections, there are three distinct zones: a dilute central zone (i.e., a zone where the particle concentration is very low, and consequently its velocity is high, that extends from the radial centre (*r = 0*) to approximately *r = 0.2 m*; an intermediate zone with a moderate particle velocity (approximately between r = *0.2 m* and *0.4 m*); and a wall zone with a low particle velocity that extends from approximately *r = 0.4 m* to *1.0 m*.

Fig 6 shows the time-mean two-phase vertical velocities at riser length z = 0.95m. The velocity profile was over-predicted and the downward flow of the particles along their carrier gas near the wall is predicted, although the no-slip boundary will guarantee a zero value for gas velocity at the immediate wall position. Fig 7(a) show the contour plot of FCC solid particles in the riser system. While Fig 7(b) represents the contour plot of single (ideal gas) phase flows including the upper and bend of the riser system. The nature of the flow field and the granular flow velocity can be seen from the contour plot. Figs. 10-11 shows the profiles of velocity in the dense region (z = 0.95 m and 2.59 m) of high solids concentration. It can be observed that inviscid model has quantitative behaviour in the constant coefficient Newtonian model, but this behaviour is inverted closer to the wall. This is also in good agreement with [1]. The deviation comparison of the predictions and experimental study observed in Fig 8 is about 0.05%.

Fig 11 show the under-predicted FCC solid velocity profile when compared with the experimental data. By observation, it can be seen that the computation was almost at the fully developed flow level between the plane z = 0.95 m and z = 2.59 m. Figs 12 and 13 show a more pronounced under-predicted model when compared with experimental result [1]. The deviation is about 5.2% at this region. Since various issues like: the grid dependency, turbulent model, discretization scheme and power law equation was resolved. The discrepancies might be on CFD error and/or error from the experimental data used. The model predicted has shown a uniform distribution of FCC solid particle along the length of the riser. The numerical results are in good agreement with the experiment, both in form and magnitude.

4.3.1 Case 1: Ug = 3.5m/s at Gs = 100 kg/m^{2}s

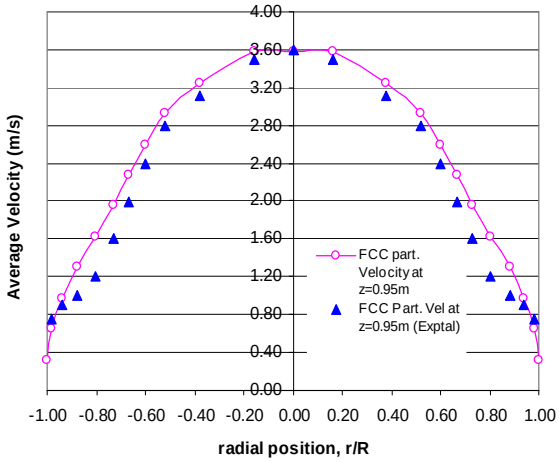

Fig 10. FCC Particle velocity profile at z =0.95m

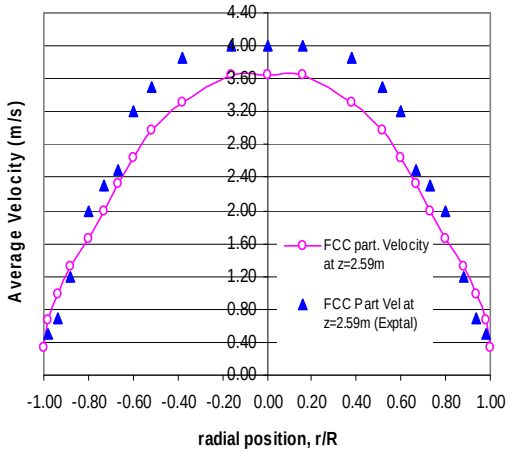

Fig 11. FCC Particle velocity profile at z =2.59m

The solids flow can be considered as fully developed if the radial solids distribution no longer changes with respect to the axial location. With this principle, it is seen that increasing

the superficial gas velocity accelerates the flow development in Figs 12, 14, 16 and 18. Again, when the solid circulation rate was increased form 3.5 m/s at 100 kg/m^{2}s to 5.5 m/s at 100 kg/m^{2}s, the flow development are lower and the simulation comparison with the experimental case can be seen in Figs. 13, 15, 17 and 19. In this figures, the predictions of the local solid volume fraction are successful. The reported profile in this study are at different riser heights: 0.95 m, 4.51 m, 10.0 m and 14.08 m. respectively. At all the bed heights in this Figs. 13, 15, 17 and 19, the core–annulus flow were closely predicted. This comparisons also provide the model validation axially [17].

Fig 19 shows a symmetrical particle velocity profile; this is a proof of transient solution to the simulation case. But when the transient simulation was carried out, the results obtained was a constant values at all level of flow in the riser system. At this point we can conclusion that the simulation was a transient case as initially viewed to be steady state. But furthermore there is a need to incorporate a user-define subroutine to address the discrepancies from the default setting. Since the phenomenological model 535 centipoises solid viscous was applied, effort will be is place to look at the viscosity predictions. Again, as the level of dilution is high, the kinetic theory of granular flow (KTGF) is underpredicting the collisional viscosities, hence the flatter velocity profile. This indicates a modelling deficiency of the KTGF in the dilute limit, which will improve when we consider larger solids loadings.

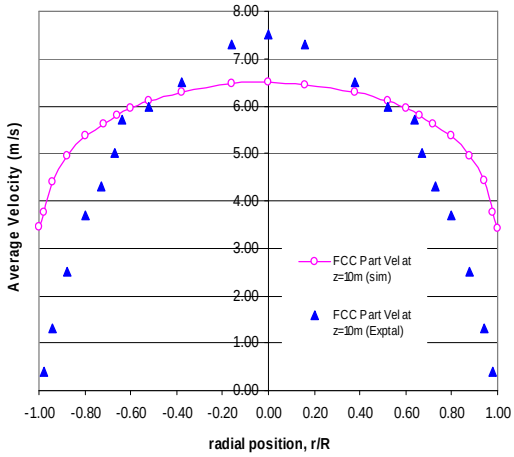

Fig 12. FCC Particle velocity profile at z =10m

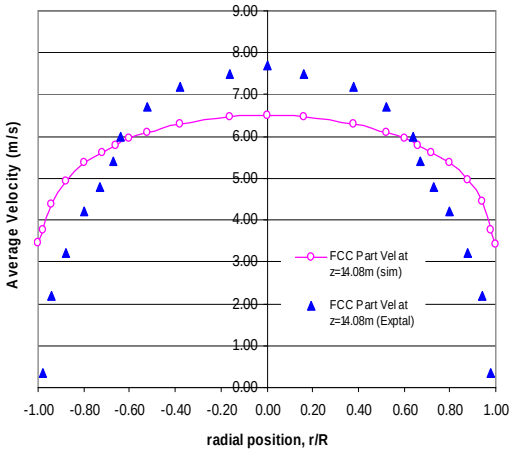

Fig 13. FCC Particle velocity profile at z =14.08m

4.4 Solid phase volume fraction distribution

It has been seen in Figs 14, 16, 18 and 20 that the solids concentration in the riser centre remains almost constant throughout the riser under each operating condition. These figures shows that even with the change in operating conditions, the solids concentration seem to remain unchanged within the operating conditions. Therefore, the flow development in the riser mainly depends on the solids distribution in the wall region. Figs 14 and 16 show a close comparison with the experimental data, but the effect toward the riser wall is a little higher than that of experimental data. Fig 19 shows good comparison of a symmetrical profile of solids holdup. Also Fig 21 shows a close and more in symmetric comparison of volume fraction when compared with the experimental data [6]. The wall effect is much noticed to be better predicted at the plane z = 10.0 m and z = 14.08 m. This may be as a result of fully developed flow along the riser length at that region.

Detail knowledge and understanding of the solids distribution is very vital for the design, development and operation of CFB/FCC riser reactor. Gas and solid particle residence time distributions in the riser, the rate of heat transfer and erosion rates of surfaces in fluidised riser beds also depend on solids volume fraction distributions. The solid particles are entrained up in column, against the gravitational acceleration, by the upflowing gas phase [17].

4.3.2 *Case 2: Ug = 5.5m/s at Gs = 100 kg/m^{2}s*

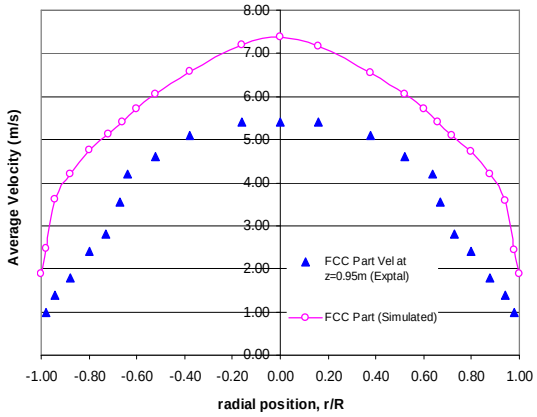

Fig 14. FCC Particle velocity profile at z =0.95m

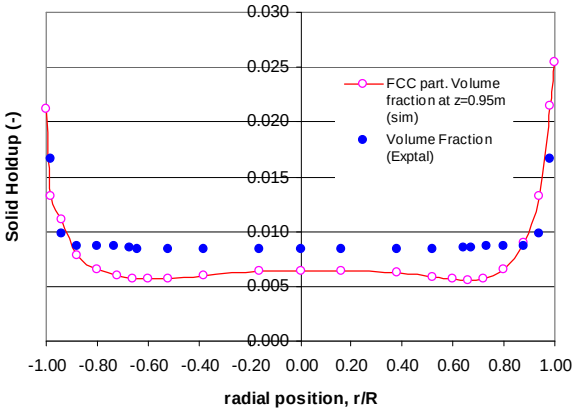

Fig 15. FCC Volume fraction at z = 0.95m

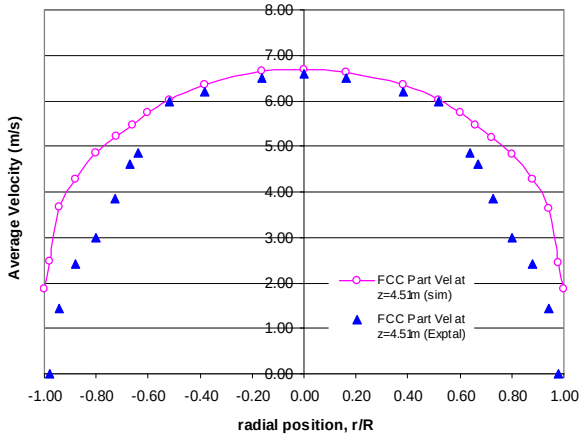

Fig 16. FCC Particle velocity profile at z =4.51m

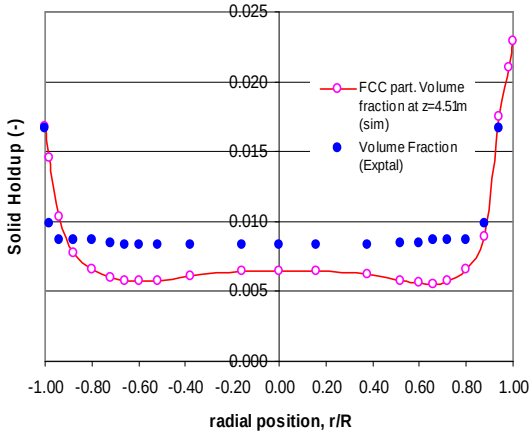

Fig 17. FCC Volume fraction at z = 4.51m

4.5 *Influence of wall restitution coefficient*

In this simulation, it is possible to investigate the influence of the restitution coefficient of the wall on the simulation results. But the default settings used is not showing enough boundary effect toward the wall of the riser. The knowledge of restitution coefficient of the wall is therefore necessary for a correct application of the model. [12] estimated the restitution coefficient of the wall from measurement of granular temperature and solid volume fraction in the dilute regime of a CFB/FCC riser.

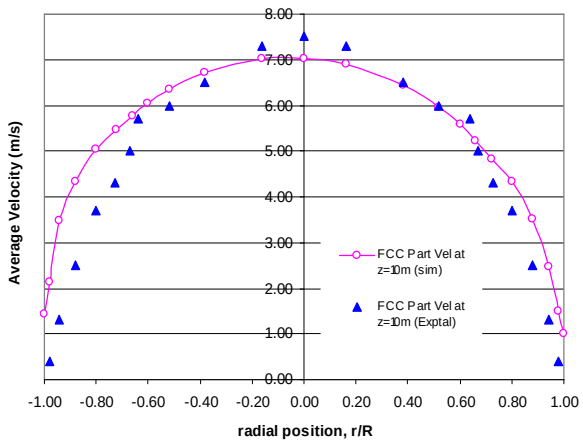

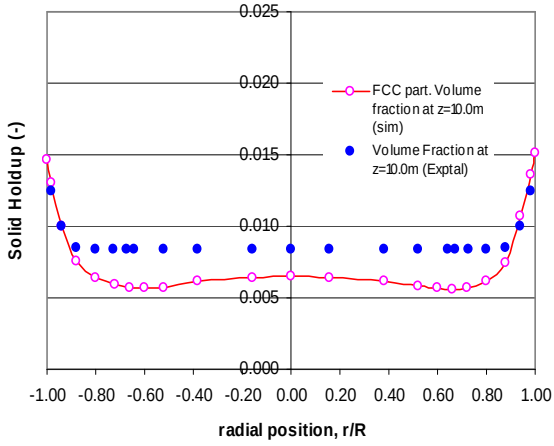

Fig 18. FCC Particle velocity profile at z =10m

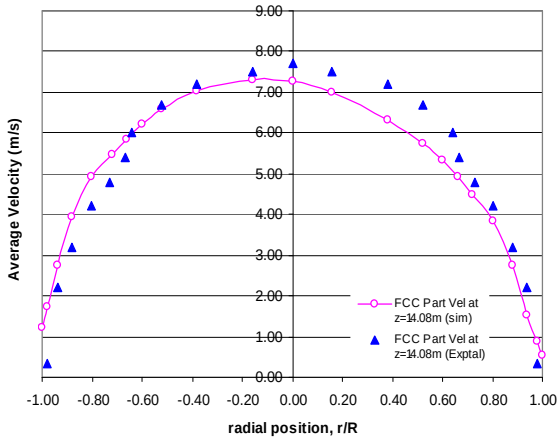

Fig 19. FCC Volume fraction at z = 10m

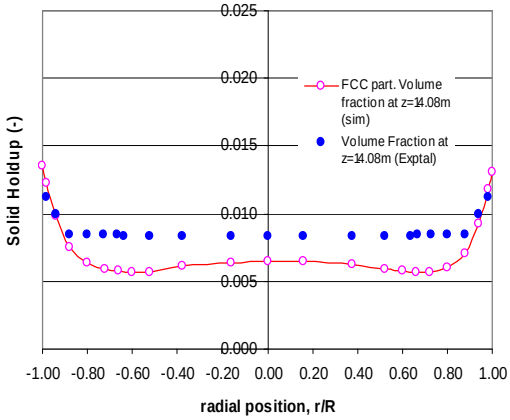

Fig 20. FCC Particle velocity profile at z =14.08m

Fig 21. FCC Volume fraction at z = 14.08m

4. Conclusion

A computational fluid dynamics study was done using a commercial code ANSYS CFX 11.0 to describe the hydrodynamic behaviour of gas-solid flow in a FCC/CFB riser. The model was based on Eulerian-Eulerian two-fluid modelling approach, incorporating the kinetic theory constitutive model for a dilute assemblies of the particulate solid, a Gidaspow's drag model for gas-particles interaction. The simulation model takes into account the axial and radial distribution of voidage, velocity and pressure drop for gas and solid phase, and solids volume fraction and particle size distribution for solid phase. The typical flow patterns of the CFB/FCC bed were obtained and compared favourably with the reported experimental results. This model results are compared with and validated against atmospheric cold bed CFB units' experimental data given in the literature for axial and radial distribution of void fraction, solids volume fraction and particle velocity, total pressure drop along the riser height and radial solid flux. The discussions of results were based on the predicted numerical results of gas-solid behaviour in the riser simulation using default setting. The kinetic theory of granular flow model applied in this simulation based on default settings, increases the instability of the Eulerian-Eulerian calculation.

The trends of the flow development are observed from axial and radial solids concentration and particle velocity distributions. For the setup operating boundary conditions, the solids concentration in dilute phase are relatively constant at the riser centre throughout the FCC riser. This is why the argument for the quick solids flow development in the riser centre. However, the flow development in the wall region is quiet slow with the solids holdup near to the riser wall decreasing slowly toward the riser height.

This discrepancies is not only explained by the particle-based approach used in this model, because of the consideration of cluster effect based on drag coefficient, this situation is initiated by the fact that the solids are accelerated to an upward velocity, and there is a very large voidage gradient in the riser bottom.

More so, increasing the overall solids circulation rate, Gs, decreasing the superficial gas velocity, Ug, increases the solids holdup in the wall region throughout the FCC riser length. In conclusion, the simulation results are in close comparison with the experimental data, although there are noticeable under-predictions and deviations which may be corrected using applied user-subroutines in the ANSYS CFX software. The overall flow patterns within the riser bed were predicted well by the model. For volume fraction around 2-3%, which is the average particle concentration in the riser system, the computed solid-holdup agrees with the experimental measurements.

Notation

c	Fluctuating velocity, m/s
C_D	Drag Coefficient
d_p	Particle diameter
g	gravitational constant, 9.81m/s^2
P	Fluid pressure
P_s	Particle pressure
$\bar{R}$	Gas constant, J/mol.K
Re	Reynolds number
r_{coeff}	Coefficient of restitution
$\vec{R}_{gs}$	Drag force between gas and particulate phases, N/m^3
t	time, s
$\vec{v}_g$	The gas velocity, m/s
$\vec{v}_g$	The gas velocity, m/s
$\vec{v}_s$	The solid velocity, m/s
$\vec{v}_{gs}$	The drift velocity, m/s
$\vec{v}_\varphi$	Velocity of phase φ, m/s
x, y	radial coordinates, m
z	axial coordinate, m

Greek letters

e_g	Gas volume fraction
e_g	solid volume fraction
e_φ	volume fraction of phase φ
$\varepsilon_{s,\max}$	maximum volume fraction of particle
Θ_s	Granular temperature, m^2/s^2
λ_s	shear bulk viscosity
μ_g	gas dynamic viscosity, kg/ms
μ_s	Solid shear viscosity, kg/ms
ρ_g	Gas density, kg/m^3
ρ_s	Solid density, kg/m^3
ρ_φ	Density of phase φ, kg/m^3

Subscripts

g	gas phase
k	turbulence kinetic energy
max	maximum
s	solid phase
CFB	Circulating fluidised bed
FCC	Fluid catalytic cracking riser
KTGF	Kinetic theory of granular flow

Acknowledgement

The authors would like to acknowledge the support from the Petroleum Technology Development Fund (PTDF), Abuja, Nigeria, for the sponsorship of this Ph.D. research study at the University of Leeds, United Kingdom and to present this paper at the 100-years centenary of AIChE in Philadelphia, USA.

References

1. Levenspiel, O. (1999) *'Chemical Reaction Engineering'* 3rd Edition John Wiley & Sons
2. Jiradilok, V., Gidaspow, D., Damronglerd, S., Koves, W. J., and Mostofi, R., (2006) *'Kinetic theory based CFD simulation of turbulent fluidization of FCC particles in riser'* Chemical Engineering Science 61, 5544-5559
3. Grace, J. R., (2000) *'Reflections on turbulent fluidization and dense suspension upflow, Powder Technology'* 113, 242-248
4. Du, B., Warsito, W., Fan, L. S., Bed, (2003) *'Nonhomogeneity in turbulent gas-solid fluidization'*, A.I.Ch.E Journal 48, 1896-1909
5. ANSYS CFX (2006) *Solver Theory Guide*. ANSYS CFX Release 11.0: 1996 ANSYS Europe, Ltd
6. Huang, W., Yan, A., and Zhu, J., (2007) *'Hydrodynamics and flow development in a 15.1m Circulating Fluidised Bed Riser'*, Chem. Eng. Techno. 30, No. 4, 460-466
7. Ding, J and Gidaspow, D., (1990) *'A bubbling fluidisation model using theory of granular flow'* AIChEJ. 36 pp. 523 – 538
8. Yang, N., Wang, W., Ge, W., Wang, L., Li, J., (2004) ,*Simulation of heterogeneous structure in a circulating fluidised-bed riser by combining the two-fluid model with EMMS approach.* Industrial and Engineering Chemistry Research 43, 5548-5561
9. Versteeg H. K., and Malalasekera W., (2007) *'An Introduction to Computational Fluid Dynamics: The Finite Volume Method'* 2nd Ed., Pearson Prentice Hall, Harlow, England.
10. Yi Cheng et al (2008) *Downer reactor: From fundamental study to industrial application*, Powder Technology 183: 364-368
11. Gidaspow, D., (1994) *Multiphase Flow and Fluidization: Continuum and Kinetic Theory Descriptions,* Academic Press, New York
12. Gidaspow, D., AND l. Huilin, (1998) *'Equation of State and Radial Distribution Function of FCC Particles in a CFB'* AIChE J., 44, 279
13. Ranade V. V (1999) *Modelling of Gas-Solid Flow in FCC Riser Reactors: Fully Developed Flow*, 2nd International Conference on CFD in Materials and Process Industries, CSIRO, Melbourne, Australia.
14. Yang, Y. I., (1991) .,*Experimental and theoretical studies on hydrodynamics in cocurrent upflow and downflow circulating fluidized beds*, PhD. Diss., Tsinhua University, Beijing, China.
15. Derouin C, et al (1997) *Hydrodynamics of Riser Units and Their Impact on FCC Operation*. Ind. Eng. Chem. Res. 36, 4504-4515
16. Martin, M. P et al (1992) *Catalytic Cracking in Riser Reactor: core annulus and elbow effects*. Chem. Eng. Sci. 47, 2319
17. Gungor A., AND Eskin N., (2007) *Hydrodynamic modelling of a circulating fluidised bed' Powder Technology* 172 p1-13